JOURNAL OF MATERIALS SCIENCE 15 (1980) 431–437

Liquid spreading on rough metal surfaces

J. F. OLIVER*, S. G. MASON
Pulp and Paper Research Institute of Canada, and Department of Chemistry, McGill University, Montreal, Canada

The influence of surface roughness on the equilibrium spreading of liquids on aluminium and stainless steel surfaces with well-characterized rough machine finishes and a well-defined technique of attaining liquid drop equilibrium has been experimentally studied. The surfaces were prepared under practical conditions, i.e. without rigorous purification or attempting to eliminate anisotropy or microheterogeneities in surface-free energy. Depending on the type of roughness, i.e. spiral-grooved, radial-grooved and porous, the advancing contact angle was in approximate agreement with one of the classical contact angle/surface roughness equations. Capillary channelling along machine grooves profoundly affected the spreading and wetting behaviour and was highly dependent on the orientation and texture of roughness. Although the observed spreading was generally smooth on all surfaces it was probable that microscopic surface asperities produce small-scale non-equilibrium contact line movements and are responsible for the extensive wetting hysteresis during drop retraction.

1. Introduction

From measurements of the spreading coefficients of liquids on water and mercury, Harkins and Feldman [1] concluded that all liquids should spread spontaneously on clean metal and other high melting-point solids with high surface-free energies, i.e. ranging from 100 to several thousand $\mathrm{mJ\,m^{-2}}$. However as was recently reported by Schrader [2] these circumstances only apply to ultra-clean surfaces prepared in an ultra-high vacuum. Under more "practical" conditions all so-called high-energy surfaces, because of their extreme susceptibility to atmospheric contamination, are rapidly converted to low-energy surfaces with surface-free energies ranging from 20 to $100\,\mathrm{mJ\,m^{-2}}$. Consequently, as found from the extensive studies of Fox *et al.* [3], with a few exceptions, wetting of high-energy solid surfaces invariably produces incomplete spreading and non-zero contact angles.

In a recent study on wetting hysteresis on low-energy surfaces using various model roughnesses, Oliver *et al.* [4] have demonstrated that depending on the type of roughness one may approximate θ_a, the advancing contact angle, with the classical contact angle/surface roughness equations of either Wenzel [5], Shuttleworth and Bailey [6], or Cassie and Baxter [7]. We have also found that these correlations apply reasonably well on surfaces of various high-energy solids with similar roughness. We should emphasize, however, that these surfaces are prepared under "practical" conditions, i.e. without rigorous chemical purification, and have oxidized surfaces which are susceptible to adventitious contamination, e.g. adsorption of organic substances present in air. Furthermore, they are neither energetically homogeneous or isotropic. We believe, however, that most of the deviations from ideal wetting behaviour, such as hysteresis are attributable to surface roughness.

2. Theory

Wenzel's equation is

$$\cos\theta = \bar{\sigma}\cos\theta_e, \qquad (1)$$

where θ and θ_e are the apparent and thermodynamic equilibrium contact angles, and $\bar{\sigma}$, the

---

*Present address: Xerox Research Centre of Canada, 2480 Dunwin Drive, Mississauga, Ontario L5L 1J9.

0022–2461/80/020431–7$02.70/0

roughness parameter, is the average ratio of the true to apparent data. Equation 1 is a thermodynamic relation, and thus implies reversibility of contact line movement, i.e. zero contact angle hysteresis; Huh and Mason [8] and Oliver *et al.* [4] have shown both theoretically and experimentally it applies to solid surfaces with no spreading energy barriers such as radial grooves.

On surfaces with parallel grooves, Shuttleworth and Bailey proposed that the apparent advancing and receding contact angles for spreading perpendicular to the grooves are respectively:

$$\theta_a = \theta_e + \phi_m, \tag{2a}$$

$$\theta_r = \theta_e - \phi_m, \tag{2b}$$

where ϕ_m and ϕ'_m are the maximum slope angles of the respective groove faces in the receding and advancing directions of the contact line. Recent theoretical calculations by Huh and Mason [8] who extended Shuttleworth and Bailey's proposals to concentric-grooved surfaces, agree reasonably well with the spreading behaviour of an advancing drop on spiral-grooved low-energy Teflon surfaces [4].

Finally for *composite* surfaces, where air is entrapped between liquid and solid, Cassie and Baxter, from considerations similar to Wenzel's, derived the equation:

$$\cos\theta = f_1 \cos\theta_e - f_2, \tag{3}$$

where f_1 and f_2 are the area fractions of solid–liquid and liquid–air interfaces respectively.

As we report below for liquids with $\theta_e < 90°$, wetting on a metal surface may increase or decrease, i.e. θ_a decrease or increase, depending upon the type of roughness.

3. Experimental procedure

The experiments were conducted in a Plexiglas cell [4] inside which discs prepared with various roughnesses could be accurately levelled and the movement of spreading liquid drops photographically recorded horizontally and vertically through optical glass windows. The cell was located in a laboratory controlled at 20 ± 1° C and temperature variations within the cell during a single experiment never exceeded ± 0.1° C. Advancing liquid drops were slowly formed at a constant flow rate between 0.007 and 0.03 $\text{cm}^3\ \text{min}^{-1}$ through a small central hole in the disc by means of a precisely controlled syringe infusion-withdrawal pump. After the drop was advanced, flow was stopped 2 to 3 min and then reversed at the same time. Horizontal photographic images of spreading drops (analysed on a Nikon Shadowgraph) were used to measure values of: (i) advancing and receding contact angles θ_a and θ_r; (ii) the contact line radius r; and in addition, (iii) values of $\Delta\theta$ and Δr, the corresponding changes in θ_a and r just before reversing the flow. Based on the analysis of at least twenty photographs recorded at different stages of advance or retraction, an overall mean value, $\bar{\theta}_a$ or $\bar{\theta}_r$ was calculated, yielding an average deviation $\leqslant 2.5°$ on all surfaces. Values of θ_a, θ_r and r were plotted against the measured volume V and the graphs were used to estimate values of the contact angle hysteresis, $H \equiv \theta_a - \theta_r$ and the drop volume hysteresis E, which we define as $E \equiv (V_a - V_r)/V_a$, where V_a and V_r are the respective volumes of advancing and receding drops at a given r [4].

Based on a method similar to that used by Champion *et al.* [9] for studying the wetting of aluminium oxide by molten metals, tracings from vertical photographic images of contours of the advancing and receding contact line provided a particularly useful and sensitive means of qualitatively mapping the spreading behaviour.

The discs were machined from 6061-T6 aluminium (nominal composition: Mg = 1%, Si = 0.6%, Cu = 0.25%, Cr = 0.25%; balance Al) with the following finishes: (i) spiral grooves – formed by lathe-machining; (ii) radial grooves – formed on a universal-grinder; and (iii) "smooth" surfaces – produced by polishing with 0.3 μm alumina abrasive on a fine nylon lapping-cloth. In addition, a 316 stainless steel sheet (nominal composition: C = 0.08%, Mn = 2.00%, P = 0.045%, S = 0.03%, Si = 1%, Cr = 16/18%, Ni = 10/14%, Mo = 2/3%, Cu = 0.5%; balance Fe (manufacturer: Buckbee Mears Co, St Paul, Minn.) etched with ~ 300 μm circular holes, spaced ~ 60 μm apart and mounted on a Teflon disc to prevent liquid penetration, was used to provide a model composite solid–liquid–air interface.

The surface profiles were examined by scanning electron microscopy (SEM) and the roughness was measured by profilometry as before [4]. Prior to each experiment the surfaces were cleaned in boiling benzene following a procedure similar to that adopted by Fox *et al.* [3]. The properties of the various liquids studied are given in Table I (footnote).

TABLE I *Summary of experimental data*

System	Solid/liquid	Roughness parameters				$\bar{\theta}_a$ (deg.)		$\bar{\theta}_r$ (deg)	H (deg)	E	$\Delta\theta$ (deg)	Δr (cm)
			$\bar{h}$ (μm)	ϕ_{rms} (deg)	$\bar{\sigma}$	expt.	calc.					
1	Aluminium/ethylene glycol (A)	Polished	$\leqslant 0.5$			61.0 ± 1.9 (55.9)*		32.2 ± 0.2	29.6 – 47.5	0.56 – 0.82	– 5.1	0.0070
7		Radial	1.2	5.2	1.003	62.0 ± 1.6 (47.7)§	55.8†	30.1 ± 2.4	50.0 – 55.7	0.90 – 0.95	– 14.3	0.0280
3		Spiral: fine	$\leqslant 0.3$			57.0 ± 1.6 (55.7)§		31.1 ± 1.0	26.0 – 48.2	0.82 – 0.91	– 1.3	0.0070
4		Spiral: medium	0.9	11.2	1.015	63.7 ± 1.1 (62.7)§	71.7‡	~ 0	$\sim \bar{\theta}_a$	1	– 1.0	0.0095
6		Spiral: coarse	2.4	7.4	1.007	69.8 ± 2.0 (65.9)§	66.4‡	~ 0	$\sim \bar{\theta}_a$	1	– 4.3	0.0125
2	Aluminium/silicone oil (B)	Polished				14.0 ± 0.9 (6.2)*		~ 0	$\sim \bar{\theta}_a$	1	– 7.8	0.1010
8		Radial				21.9 ± 3.2 (6.5)§	4.5†	~ 0	$\sim \bar{\theta}_a$	1	– 15.4	0.0270
5		Spiral (medium)				28.1 ± 2.5 (11.5)§	22.0‡	~ 0	$\sim \bar{\theta}_a$	1	– 16.6	0.0300
9	Stainless steel/ ethylene glycol (A)	Polished				60.2 ± 1.6*		31.5 ± 1.0	28.7 ± 1.6		– 2.5	0.007
10		Orthogonal array of holes				106.7 ± 3.6	109.7¶	~ 0	$\sim \bar{\theta}_a$	~ 1	– 5.0	0.021

* Assumed = θ_e.

† Calculated from Equation 1 using measured $\bar{\sigma}$.

‡ Calculated from Equation 2a with $\phi_m = \sqrt{2}\, \phi_{rms}$ [4].

§ Modified advanced contact angle, $\theta'_a \equiv \bar{\theta}_a + \Delta\theta$ after stopping flow.

¶ Calculated from Equation 3 using measured $f_1 \doteq 0.443$ and $f_2 = 0.557$.

Physical properties of liquids (measured at 20° C):

(A) ethylene glycol + 0.075 wt% dye (eosin B): surface tension $\gamma = 46.8\,\mathrm{mN\,m^{-1}}$; density $\rho = 1.1\,\mathrm{g\,cm^{-3}}$; viscosity $\eta = 20\,\mathrm{Pa\,sec}$;

(B) silicone oil DC702 (Dow Corning) + 0.015 wt% dye (calco oil): $\gamma = 29.3\,\mathrm{mN\,m^{-1}}$; $\rho = 1.07\,\mathrm{g\,cm^{-3}}$; $\eta = 42\,\mathrm{Pa\,sec}$.

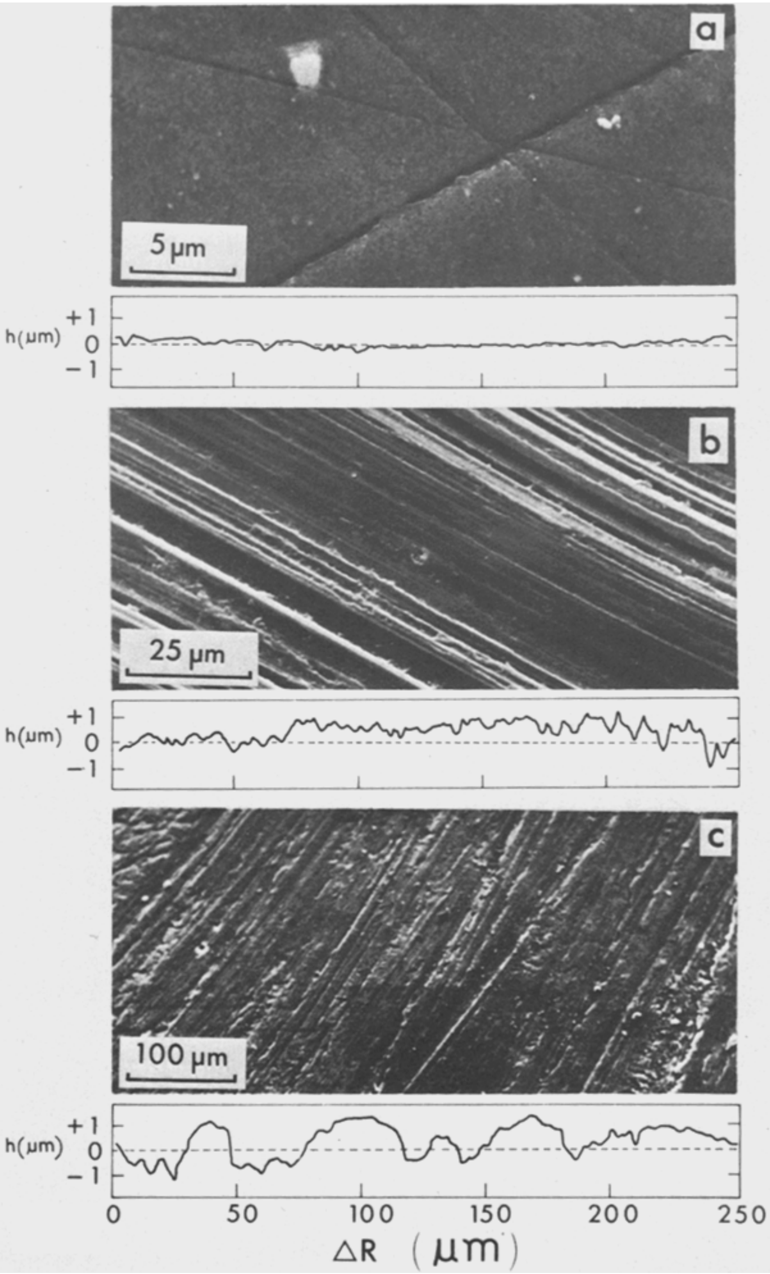

Figure 1 SEMs and corresponding profilograms of various machined aluminium surfaces: (a) polished, showing random microscopic grooves $< 0.5\,\mu m$ wide and deep; (b) lathe-machined, which approximate concentrically grooved model roughness; and (c) machine-ground, which approximate radially grooved model roughness.

4. Results and discussion

4.1. Spreading on roughened aluminium surfaces

SEM-graphs of the various aluminium surfaces studied along with corresponding profilograms are shown in Fig. 1. Estimated values of the various roughness parameters used to characterize the surfaces are given in Table I. Quantitative differences in spreading behaviour of ethylene glycol and silicone oil were compared by means of plotting variations in θ and r on increasing and then decreasing V (Figs. 2 and 3) and mapping the development of contact line contours (Fig. 4).

On the polished (systems 1 and 2) and radial-grooved (systems 7 and 8) surfaces the advancing contact line movement appeared fairly smooth and asymmetric. Drop advance on the spiral grooves (systems 3, 4, 5 and 6) was also asymmetric and there was little or no indication of stick–jump movements [8] of the contact line, as was pre-

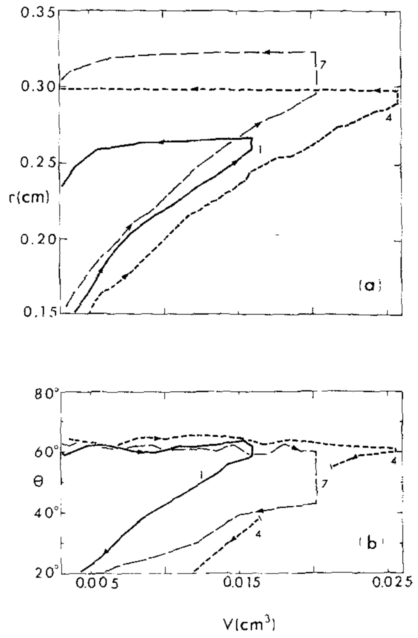

Figure 2 Effect of roughness on the spreading of ethylene glycol for polished (system 1), spiral-grooved (system 4) and radial-grooved (system 7) aluminium surfaces, expressed as the variations with V of (a) the contact line radius, r; and (b) the apparent contact angle, θ.

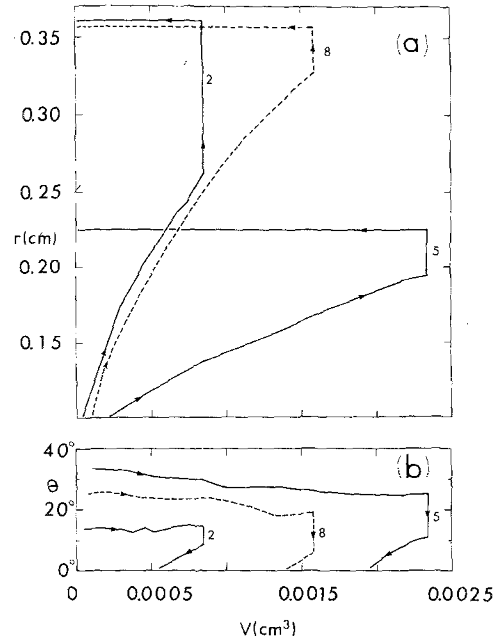

Figure 3 Effect of roughness on the spreading of silicone oil for polished (system 2), spiral-grooved (system 5) and radial-grooved (system 8) aluminium surfaces, expressed as the variations with V of (a) the contact line radius, r; and (b) the apparent contact angle, θ.

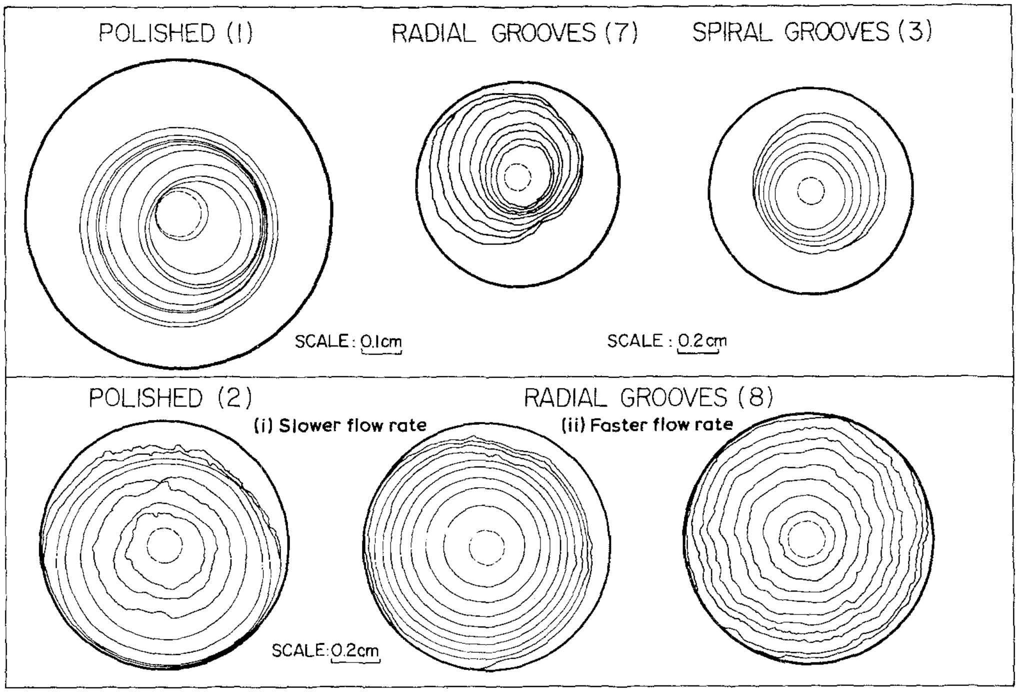

Figure 4 Comparison of the effect of roughness on contact line contours for ethylene glycol (upper) and silicone oil (lower) drops advancing on various aluminium surfaces, for systems (numbered) given in Table I. The two tracings for system 8 show the effect of liquid flow-rate on contact line development. The lower rate (i) corresponds to 0.007 cm^3 min^{-1} and the higher rate (ii) to 0.03 cm^3 min^{-1}.

viously observed [4] on Teflon surfaces with similar roughness, presumably because of the higher wetting and increased spreading along, rather than across, the grooves. However, since surface asperities $< 0.05\,\mu$m high have been found to inhibit spreading significantly [10], non-equilibrium jumps of this order are conceivable.

With increased wetting the very similar rate of development of r (Fig. 3) for the polished (system 2) and radial-grooved (system 8) surfaces compared to the spiral grooves (system 5) offered no more resistance to spreading than the polished surface. However, in an experiment performed at a higher drop flow rate on the radial grooves, the contact line contours (Fig. 4) consistently appeared polygonal-shaped, reflecting inconsistencies in groove dimensions; in the deeper grooves, capillary channelling resulted in fingers of liquid extending about 0.1 cm ahead of the drop. The slightly eccentric and wavy contact line contour development on the polished surface (Fig. 4) also suggests that the presence of fine microscratches (see Fig. 1a) can influence spreading behaviour significantly, particularly with the higher wetting liquid. The extent of this capillary channelling on machined metal surfaces is highly dependent on the orientation and texture of the roughness, as was found by Parker and Smoluchowski [11], Bikerman [12], Bascom *et al.* [13] and more recently demonstrated by Patrick and Brown [14] and Oliver *et al.* [10, 15] using an involatile liquid in an SEM.

As a result of this slow capillary channelling we observe that values of Δr and $\Delta\theta$ (Table I) indicate a considerable lag in spreading equilibrium. With increased wetting, i.e. lower θ_e, this effect increased and the values of Δr suggest that the random and intersecting grooves of the polished surface (see Fig. 1a) inhibit spreading more than either the radial or spiral grooves.

Obviously with these systems one can no longer assume quasi-equilibrium spreading [8]. To offset this complication we have considered $\theta'_a \equiv \theta_a + \Delta\theta$ as the steady-state value and assumed that $\Delta\theta$, caused by the lag in spreading equilibrium, is approximately constant throughout the drop advance. On this basis and using the values of $\bar{\sigma}$ obtained from profilometry it can be seen from Table I that for the radial grooves (systems 7 and 8) assuming $\theta_e = \theta'_a$ for the polished surface, Equation 1 holds reasonably well. In contrast, on the spiral grooves (systems 3, 4, 5 and 6) the roughness produced an increase in θ'_a, which for the coarser surface (system 6) based on the measured ϕ_{rms} (Table I), was in approximate agreement with Equation 2. Not surprisingly, on the fine surface (system 3), where $\bar{h}$ was much the same as for the polished surface, θ'_a was the same. The higher $\bar{\theta}_a$ value on the polished surface must have resulted from the more irregular grooving and hence slower capillary channelling.

On retraction, the much higher wetting, especially with silicone oil, resulted in extensive sticking on all these surfaces with little or no contact line recession, as indicated by the large values of E and H (derived from Figs. 2 and 3) given in Table I. Although surface heterogeneities are likely to contribute to these values, previous investigations in our laboratories, particularly on the edge effect [16, 17], strongly suggest that in these systems roughness plays the major role in causing discrepancies from predicted behaviour.

4.2. Spreading on porous stainless steel

During drop advance this surface (see Fig. 5) produced distinct and regular stick–jump movements [8], the largest of which (as shown in Fig. 6) resulted in an increase in r of 160 μm and an accompanying decrease in θ_a of 10°. With increasing V the frequency and size of these jumps decreased while the contact line tended to align with the orthogonal array of holes and retain a slightly non-circular shape with the ratio of the largest to the shortest r varying from 1.0 to 1.2.

For small drops, i.e. $r < 0.12$ cm, θ_a varied

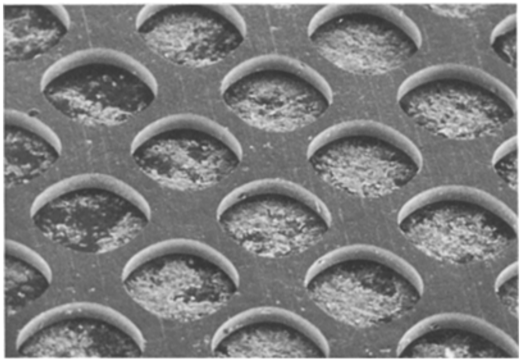

Figure 5 SEM of a stainless steel mesh made up of an orthogonal array of approximately circular 280 μm diameter holes, which entrap air with the lower wetting liquid (system 10, Table I) forming a model composite surface.

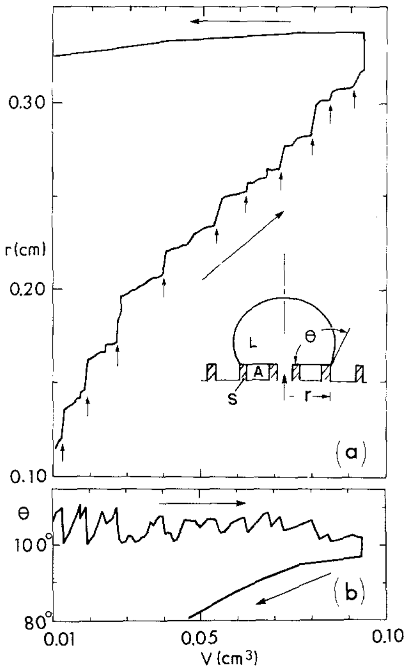

Figure 6 Effect of roughness on the spreading of ethylene glycol for a stainless steel mesh comprising of an orthogonal array of holes (system 10) which form a model composite, solid (S)–liquid (L)–air (A) interface. (a) Contact line radius, r; and (b) contact angle, θ. Vertical arrows indicate the more pronounced contact line jumps.

depending on the direction of observation, but only slightly for drops covering more than twelve holes. Theoretical and experimental studies on the relationship between drop size and roughness for microscopic drops on similar surfaces have been reported elsewhere [8, 10]. The value of $\bar{\theta}_a$ (Table I) for the larger drops shows good agreement with Equation 3, based on θ_a measured for the polished surface (system 9) and the measured area fractions f_1 and f_2, even though we would expect that analogous to Equation 1, Equation 3 may apply only when the liquid spreads free of non-equilibrium jumps.

The relatively large values of Δr and $\Delta\theta$ indicate slow liquid penetration into the holes. On retraction, extensive sticking of sections of the contact line occurred at the edges of holes, as a result the value of E approached unity.

5. Conclusions

These experiments demonstrate that the roughness and texture of machined metal surfaces can profoundly influence wetting and spreading of liquids. Although the approximate validity of Equations 1, 2a and 3 for $\bar{\theta}_a$ as the representative characteristic of spreading, correlates with the measured roughness in the predicted way for these model surfaces, it is evident from the observed local variations in the contact line that other roughness characteristics, such as surface texture, need to be included to give a more comprehensive description of spreading behaviour. A partial attempt in this direction was made in the theoretical study of Huh and Mason [8].

The behaviour of more typical machine finishes is likely to vary according to how closely they resemble these model surfaces, and to what extent their roughness can provide navigable channels for the liquid to spread.

Acknowledgement

The authors wish to thank A. Rezanowich and G. Seibel of PPRIC for their valuable assistance with the scanning electron microscopy.

References

1. W. D. HARKINS and A. FELDMAN, *J. Amer. Chem. Soc.* 44 (1922) 2665.
2. M. E. SCHRADER, Fluid-Solid Surface Interactions, Proceedings of the 2nd Symposium, edited by H. J. Lugt, U.S. Naval Ship Res. Dev. Cent., Bethedsa, Maryland (1974) pp. 151–67.
3. H. W. FOX, E. F. HARE and W. A. ZISMAN, *J. Phys. Chem.* 59 (1955) 1097.
4. J. F. OLIVER, C. HUH and S. G. MASON, *Colloids and Surfaces* 1 (1980) to be published.
5. R. N. WENZEL, *Ind. Eng. Chem.* 28 (1936) 988; *J. Phys. Colloid Chem.* 53 (1949) 1466.
6. R. SHUTTLEWORTH and G. L. J. BAILEY, *Disc. Farad. Soc.* 3 (1948) 16.
7. A. B. D. CASSIE and S. BAXTER, *Trans. Farad. Soc.* 40 (1944) 546.
8. C. HUH and S. G. MASON, *J. Colloid Interface Sci.* 60 (1977) 11.
9. J. A. CHAMPION, B. J. KEENE and J. M. SILWOOD, *J. Mater. Sci.* 4 (1969) 39.
10. J. F. OLIVER and S. G. MASON, *J. Colloid Interface Sci.* 60 (1977) 480.
11. E. R. PARKER and R. SMOLUCHOWSKI, *Trans. Amer. Soc. Metals* 35 (1945) 362.
12. J. J. BIKERMAN, *J. Phys. Colloid Chem.* 54 (1950) 653.
13. W. D. BASCOM, R. L. COTTINGTON and C. R. SINGLETERRY, *ACS Adv. Chem. Ser.* 43 (1964) 355.
14. R. L. PATRICK and J. A. BROWN, *J. Colloid Interface Sci.* 35 (1971) 362.
15. J. F. OLIVER, C. HUH and S. G. MASON, *J. Adhesion* 8 (1977) 223.
16. *Idem, J. Colloid Interface Sci.* 59 (1977) 568.
17. E. BAYRAMLI and S. G. MASON, *ibid* 66 (1978) 200.

Received 26 April and accepted 5 July 1979.